19th Brazilian Congress of Thermal Sciences and Engineering
November 06th-10th, 2022, Bento Gonçalves - RS - Brazil

ENC-2022-0364
THERMO-ECONOMIC ANALYSIS OF A CONVENTIONAL REFRIGERATOR HOUSEHOLD USING PCM

David Silva Ferraz
Sara Isabel de Melo Resende
Federal University of Minas Gerais, Post-Graduate Program in Mechanical Engineering.
Av. Antônio Carlos, 6627 - Belo Horizonte/MG - 31270-901 - Brazil
david-ferraz@ufmg.br
sara_sidmr@yahoo.com.br

Cleison Henrique de Paula
Federal University of Minas Gerais, School of Engineering.
Av. Antônio Carlos, 6627 - Belo Horizonte/MG - 31270-901 - Brazil
cleissonhp@yahoo.com.br

Ralney Nogueira de Faria
Federal Center for Technological Education of Minas Gerais, Campus V, UNED Divinópolis.
R. Álvares Azevedo, 400 - Bela Vista - Divinópolis/MG - 35503-822 - Brazil
ralneyfaria@cefetmg.br

Raphael Nunes de Oliveira
Federal University of Minas Gerais, School of Engineering.
Av. Antônio Carlos, 6627 - Belo Horizonte/MG - 31270-901 - Brazil
rphnunes@demec.ufmg.br

Abstract. *In Brazil, household refrigerators correspond to 30% of the average consumption of domestic electrical energy. Improving the efficiency of these equipment promotes a reduction of domestic costs with electric energy while simultaneously reducing the demand to join electric services. In 2021, Brazil went through a water crisis with a reduction in the volume of water in hydroelectric dams, implying greater participation of thermoelectric plants to avoid blackout situations. To reduce the residential demand for electricity and increase the energy efficiency of household refrigerators, this work proposes the numerical simulation of the behavior of a domestic refrigerator integrated with a PCM (Phase Change Material) positioned next to the condenser for storing energy in the form of latent heat to extend the time the compressor remains off and reduce the number of components starts. The PCM absorbs heat from the condenser during the time the compressor is running and changes from the solid phase to the liquid phase by absorbing latent heat. The thermal inertia provided by the phase change of the PCM in the condenser allows the heat exchange with the environment to be more uniform by reducing the peak temperature of the condenser during the phase in which the compressor remains on. The attenuated heat exchange provides a reduction in the temperature of the condenser and consequently promotes an increase in the energy efficiency of the refrigerator. The advantage of reducing the number of compressor starts is that the start is the moment of greatest conversion of energy into friction between the mechanical components of the compressor. Another benefit of this reduction is the extension of the compressor's lifespan. The COP calculated was 1.778, the work done by the compressor was 0.0958 kJ/s, the heat released to the PCM (condenser) was 0.266 kJ/s, the heat absorbed on the evaporator was 0.1704 kJ/s, and the PCM volume was 0.00115 m^3. The use of PCM in condensers proved to be promising and assertive for small refrigeration systems, such as household refrigerators.*

Keywords: *Household Refrigerator, Phase Change Material, PCM, Computer Simulation, Thermo-economic Analysis*

1. INTRODUCTION

According to Boeng and Melo, (2014), in Brazil, household refrigerators are responsible for 30% of the average residential electricity consumption The energy consumption of domestic refrigerators depends on the efficiency of its components (compressor, expansion valve, condenser, evaporator, and PCM - Phase Change Material), the ambient

temperature, the thermal load, the number of doors opened, the thermostat setpoint temperature, and the fluid flow that migrates from the condenser to the evaporator during the time the compressor is off (Marques et al., 2014).

Several studies and models use the PCM next to the refrigerator evaporator, on the outside, also acting as a thermal insulator for the chamber (Joybari et al., 2015). Octadecane, an alkane hydrocarbon, was chosen as PCM positioned next to the condenser in this work. Cheng and Yuan, (2013) consider the condenser as an important component and it has an important effect on thermal efficiency because all thermal load must be released to the environment through it. The PCM absorbs heat from the condenser during the time the compressor is running and changes from the solid phase to the liquid phase by absorbing latent heat. The thermal inertia provided by the phase change of the PCM in the condenser allows the heat exchange with the environment to be more uniform by reducing the peak temperature of the condenser during the phase in which the compressor remains on. It extends the time the compressor remains off, reduces the number of components starting, and promotes an extension of the compressor's lifespan because the start is the moment of greatest conversion of energy into friction between the mechanical components of the compressor (Joybari et al., 2015). According to Joybari et al., (2015), modifications on compressors or isolation modifications to improve efficiency are either costly or difficult to be applied. PCM has been considered a good way to improve it.

The R600a refrigerant has been introduced in the refrigerator market as a viable replacement for R134a because the charge required for R600a is lower than R134a, R600a is cheaper than R134a and R600a has a Global Warming Potential smaller than R134a (Joybari et al., 2013).

The purpose of this work is to perform a thermo-economic analysis of the mathematical model for a domestic refrigerator using PCM on a condenser and R600a as refrigerant fluid for further numerical optimization and improving its performance. The cost of PCM is a small proportion of the total cost of an optimized novel refrigerator (Yuan and Cheng, 2014). To develop this mathematical model has used parameters of a refrigerator brand Brastemp with a volume of 375 liters model BRM44HBANA10.

2. METHODOLOGY

To calculate the coefficient of performance (COP) is necessary to find the length of the heat exchangers and the work done by the compressor. The mathematical model was developed on EES (Equation Engineering Solver). Figure (1) shows the refrigerator divided into seven relevant points:

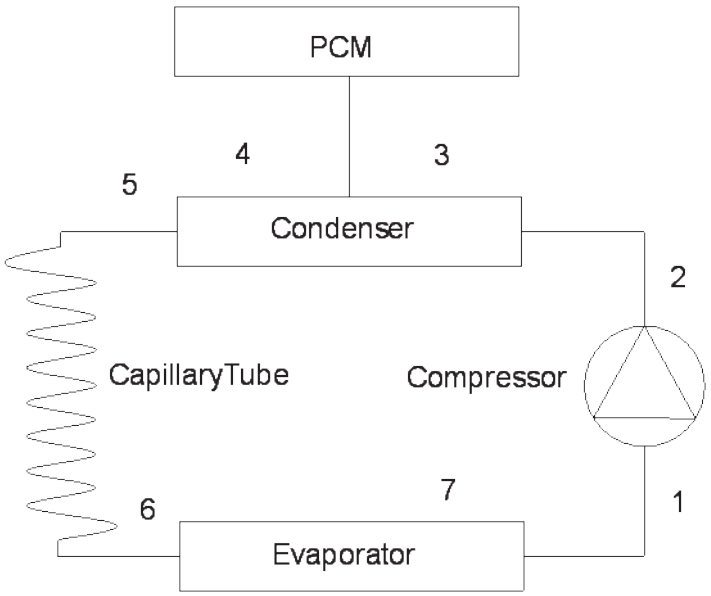

Figure 1. Domestic refrigeration system – (1) Compressor inlet / Evaporator outlet, (2) Compressor outlet / Condenser inlet, (3) Fluid liquefaction start point, (4) Fluid liquefaction endpoint, (5) Condenser outlet / Capillary tube inlet, (6) Capillary tube outlet / Evaporator inlet and (7) Fluid vaporization end region.

In this section, each part of the mathematical model was analyzed and showed the adopted considerations. An advantage of computer simulation of thermodynamic systems is the possibility of developing systems and obtaining results of their behavior before the use of prototypes and reduced costs. Figure (2) presents the block diagram used as a basis for the development of the mathematical model:

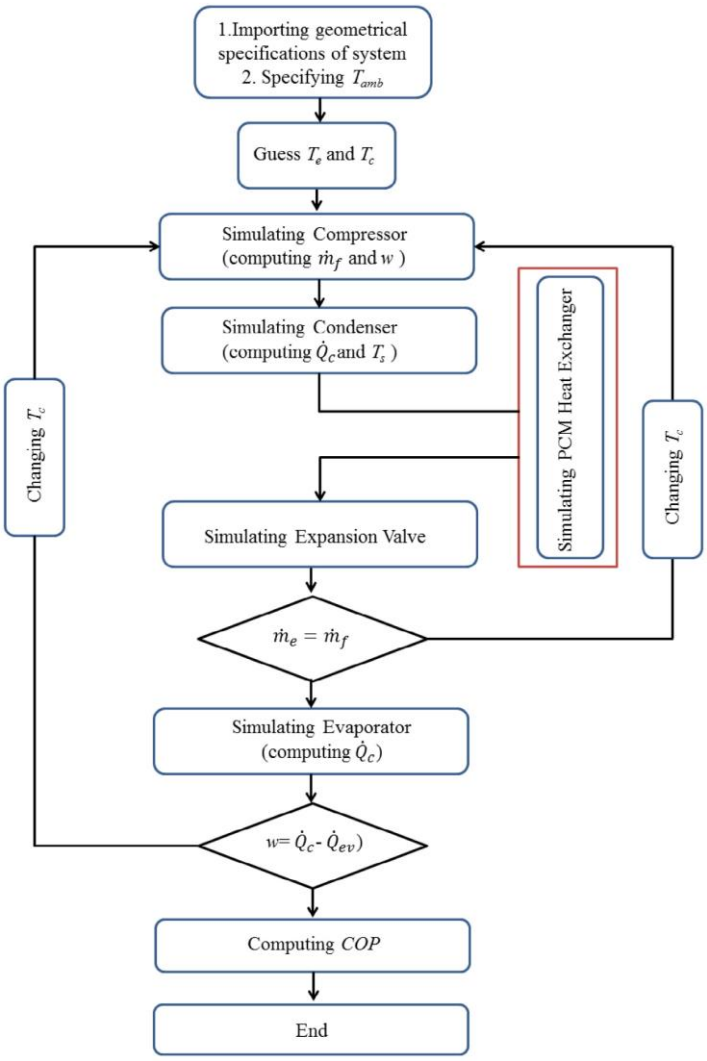

Figure 2. Simulation algorithm in refrigeration cycle utilizing PCM heat exchanger.
Available from Bakhshipour et al., (2017).

The arbitrated conditions are the condensing temperature (T_3 = 45.0°C), the environment temperature (T_{amb} = 25.0°C), the evaporator chamber temperature (T_{cha} = -10.0°C), the superheating (δ_{sup} = 7.0°C) and subcooling (δ_{sub} = 5.0°C).

2.1. Compressor

The compressor used in this article is from manufacturer Embraco, model EM2T 600CLP, used for the refrigerant fluid R600a. The reciprocating piston increases the pressure and temperature of the refrigerant fluid, pushing it through the entire circuit. The model was developed considering an adiabatic compressor, with constant volumetric and isentropic efficiencies and negligible surface heat dissipation, as proposed by Wang et al., (2007) and Bakhshipour et al., (2017). The isentropic efficiency η_{is} should be calculated from h_1 (compressor inlet enthalpy), h_2 (compressor outlet enthalpy), and h_{2is} (isentropic enthalpy):

$$\eta_{is} = \frac{h_{2\,is} - h_1}{h_2 - h_1} \tag{1}$$

The mass flow rate $\dot{m}_R$ was determined by Bakhshipour et al., (2017) from the specific mass ρ, the volumetric displacement of the compressor V_R, the volumetric efficiency η_v and the rotation "n" of the engine:

$$\dot{m}_R = \frac{\rho\, V_R\, \eta_v\, n}{60} \tag{2}$$

Considering the refrigeration circuit as intact and watertight, the mass flow rate is constant throughout the cycle and was used to calculate other parameters of the system. The volumetric efficiency of the compressor η_v is obtained from the ratio of pressures P_1 (compressor inlet) and P_2 (compressor outlet), determined by Wang et al., (2007):

$$\eta_v = 0.851 - 0.0241 \left(\frac{P_2}{P_1} \right) \tag{3}$$

The work done by the compressor $\dot{W}_{comp}$ is given by the equation:

$$\dot{W}_{comp} = \dot{m}_R \, (h_1 - h_2) \tag{4}$$

2.2. Condenser

The condenser is the component of the refrigeration cycle that performs the cooling of the fluid that arrives in the superheated vapor state at high pressure and after giving up heat to the PCM, it condenses and reaches the liquid state at high pressure. The condenser is divided into three segments: superheated vapor flow, two-phase flow, and subcooled liquid flow (Wang et al., 2007). Each of these sections has its equations and correlations. For this model, the fluid flow condition was considered one-dimensional and the heat exchange between fluid and pipe in the axial region, the thermal resistance of the pipe walls, and the pressure drop along the pipe were neglected (isobaric heat exchanger). The condensation temperature adopted is 45.0°C according to Embraco, (2022). The heat transfer rate and the total length of the condenser are the sums of rates and lengths of the sections (Wang et al., 2007):

$$\dot{Q}_{cond} = \dot{Q}_{2,3} + \dot{Q}_{3,4} + \dot{Q}_{4,5} \tag{5}$$

$$L_{cond} = L_{2,3} + L_{3,4} + L_{4,5} \tag{6}$$

2.2.1. Superheated vapor segment

For the superheated vapor segment, the heat transferred by the fluid to the PCM is obtained from the equation (Incropera et al., 2008):

$$\dot{Q}_{2,3} = \dot{m}_R \left(h_2 - h_3 \right) = H A_{2,3} \, \Delta T_{ml\,2,3} \tag{7}$$

Considering the enthalpy values h_2 and h_3, the convective coefficient H, the exchanger area $A_{2,3}$, the logarithmic mean $\Delta T_{ml\,2,3}$, and the PCM temperature constant during the phase change (Incropera et al., 2008):

$$\Delta T_{ml\,2,3} = \frac{T_2 - T_3}{ln\left(\frac{T_2 - T_{PCM}}{T_3 - T_{PCM}} \right)} \tag{8}$$

The area of the superheated vapor segment is calculated by the equation:

$$A_{2,3} = \pi \, d_c \, L_{2,3} \tag{9}$$

Where d_c is the internal diameter of the heat exchanger. Reynolds and Prandtl numbers should be calculated using values of the mass flow and the thermodynamic properties of the fluid at the inlet of the exchanger makes it possible to identify and define the most appropriate heat correlation to calculate the global coefficient and the convective coefficient.

2.2.2. Two-phase flow segment

The calculation of the heat transfer rate in the two-phase section uses the same equations for the superheated vapor section (Incropera et al., 2008):

$$\dot{Q}_{3,4} = \dot{m}_R \left(h_3 - h_4 \right) = \bar{H}_{3,4} \, A_{3,4} \left(T_3 - T_{PCM} \right) \tag{10}$$

$$A_{3,4} = \pi \, d_c \, L_{3,4} \tag{11}$$

For two-phase flow, the most appropriate correlation to calculate the overall coefficient and the convection coefficient must be determined after calculating the Prandtl, Weber, Froud, Convection, and Boiling numbers. The convective coefficient $\bar{H}$ must be obtained by calculating the average convective coefficient for different quality values, using a constant and known step size.

2.2.3. Subcooled liquid segment

The heat transfer rate in the subcooled liquid leg uses the same equations to calculate the superheated vapor segment (Incropera et al., 2008):

$$\dot{Q}_{4,5} = \dot{m}_R \left(h_4 - h_5 \right) = H_{4,5} \, A_{4,5} \, \Delta T_{ml\,4,5} \tag{12}$$

$$\Delta T_{ml\,4,5} = \frac{T_4 - T_5}{ln\left(\frac{T_4 - T_{PCM}}{T_5 - T_{PCM}} \right)} \tag{13}$$

$$A_{4,5} = \pi \, d_c \, L_{4,5} \tag{14}$$

The subcooling (δ_{sub}) is the difference between the saturation and exit temperatures of the condenser and was arbitrated at 5.0°C. Reynolds and Prandtl numbers should be calculated using values of the mass flow and the thermodynamic properties of the fluid at the inlet of the exchanger makes it possible to identify and define the most appropriate heat correlation to calculate the global coefficient and the convective coefficient.

2.3. Capillary tube

The capillary tube promotes a flow restriction in the system, due to the reduction of the cross-sectional area of the flow. Considering the watertight system, in which the mass flow rate is conserved at all points, the reduction in the area promotes an increase in the velocity of the fluid. Considering that the component does not exchange heat with the environment or other systems, the enthalpy at point (5) is equal to point (6), in an isenthalpic process (Wang et al., 2007). The capillary tube length is calculated by adding the lengths of the subcooled (*sub*) and biphasic (*tf*) sections given by Wang et al., (2007):

$$L_{cap} = \left[\frac{2 \, d_{cap} \, \Delta P}{f_{cap} \, v \, G^2} \right]_{sub} + \left[\frac{2 \, d_{cap}}{f_{cap} \, v \, G^2} \left[P_5 - P_6 - G^2 \left(v_6 - v_5 \right) \right] \right]_{tf} \tag{15}$$

Where f_{cap} is the friction factor, G is the mass velocity, P is the pressure and v is the specific volume for the fluid at the inlet (5) and outlet points of the capillary tube (6).

2.4. Evaporator

The evaporator is the component of the refrigeration cycle that heats the fluid that arrives in the two-phase state at low pressure. The evaporator is divided into two segments: two-phase flow and superheated vapor (Wang et al., 2007). Each of these sections has its equations and correlations identical to those of the condenser. For the model, the same fluid flow considerations for the condenser and the two-phase flow were considered. The most appropriate correlation to calculate the global coefficient and the convection coefficient must be determined after calculating the numbers of Weber, Froud, Convection, and Boiling. The convective coefficient $\bar{H}$ must be obtained by calculating the average convective coefficient for different quality values, using a constant and known step size.

2.5. Phase Change Material

Octadecane, an alkane hydrocarbon, was chosen as PCM positioned next to the condenser in this work. The PCM had as a criterion the proximity of its melting point (T_{PCM} of 27.2°C) with environment temperature, allowing the use of low temperature and pressure on the condenser, to reduce the work done by the compressor and reduce the upstream temperature of the capillary tube, increasing the performance of the refrigerator (Bakhshipour et al., 2017). The consideration to be carried out in this study is that the PCM maintains a constant temperature during the phase change,

like a pure substance. Only the latent heat of the PCM was considered, due to it being in phase change during the operating cycle of the equipment. The amount of energy (E) absorbed by the PCM and released environment is given by Joybari et al., (2015):

$$E = \rho_{PCM} \; V_{PCM} \; \lambda_{PCM} \tag{16}$$

Where ρ is the specific mass, V_{PCM} is the volume of the PCM and λ_{PCM} is the latent heat of the PCM. The minimum volume of the PCM must ensure that all energy released by the condenser is absorbed as latent heat on PCM during a time t_{on}, from Eq. (16).

$$V_{PCM} = \frac{\dot{Q}_{cond}}{\rho_{PCM} \; \lambda_{PCM} \, t_{on}} \tag{17}$$

2.6. Coefficient of Performance

The coefficient of performance (COP) is obtained from the ratio between the heat absorbed in the evaporator and the work done by the compressor (Sonntag and Borgnakke, 2003):

$$COP = \frac{\dot{Q}_{evap}}{\dot{W}_{comp}} = \frac{\dot{Q}_{evap}}{\dot{Q}_{cond} - \dot{Q}_{evap}} \tag{18}$$

3. RESULTS AND DISCUSSION

3.1. Compressor

The arbitrated conditions and data obtained from the manufacturer's manual allowed the calculation of the operating parameters of the refrigeration system. For the compressor, the results are shown in Table 01:

Table 01. Fluid properties at the compressor inlet (1) and compressor outlet (2).

Property	Compressor inlet / Evaporator outlet (1)	Compressor outlet / Condenser inlet (2)
Pressure (P)	72.2 kPa	604.0 kPa
Temperature (T)	-13.0 °C	75.0 °C
Enthalpy (h)	539.0 kJ/kg	675.1 kJ/kg

From the fluid properties obtained for points (1) and (2), the volumetric efficiency of the compressor (0.6493), the total mass flow rate of the system (0.0007 kg/s or 2.535 kg/h), and work done by the compressor (0.0958 kJ/s or 0.1285 hp) were determined. The model presented a result for mass flow of 4% lower than that specified in the manufacturer's manual, being a very close result. The work done by the compressor was 29% less than that specified. This difference is attributed to the consideration that the compressor would not exchange heat with the environment.

3.2. Condenser

Condensation temperature was set at 45.0°C according to Embraco, (2022) and constant pressure along the heat exchanger (isobaric). The arbitrated condenser inner diameter (d_c) was 0.003 m (Yuan and Cheng, 2014). The refrigerant fluid at point (3) was considered a saturated vapor state, at point (4) in the saturated liquid state, and at point (5) in the subcooled liquid state.

Table 02. Fluid properties at the relevant points of the condenser.

Property	Compressor outlet / Condenser inlet (2)	Point (3) Saturated vapor	Point (4) Saturated liquid	Condenser outlet / Capillary tube inlet (5)
Pressure (P)	604.0 kPa	604.0 kPa	604.0 kPa	604.0 kPa
Temperature (T)	75.0 °C	45.0 °C	45.0 °C	40.0 °C
Enthalpy (h)	675.1 kJ/kg	615.0 kJ/kg	309.9 kJ/kg	297.1 kJ/kg

3.2.1. Superheated vapor section

Convective coefficient $H_{2,3}$, exchanger area $A_{2,3}$ and length of exchanger $L_{2,3}$ were determined from the calculation of Reynolds ($Re_{c,2,3}$ = 34059) and Prandtl ($Pr_{c,2,3}$ = 0.8344), obtained from the mass flow rate and thermodynamic properties of the fluid in the heat exchanger such as specific heat ($cp_{2,3}$ = 1.997 kJ/kg-K), thermal conductivity ($k_{R2,3}$ = 0.021 W/m-K) and friction factor ($f_{2,3}$ = 0.0147). The Gnielinski correlation was chosen as the most appropriate to calculate the global coefficient and the convective coefficient, covering a wide range of Reynolds values (Incropera et al., 2008):

$$Nu_{2,3} = \frac{\frac{f_{2,3}}{8}\left(Re_{2,3} - 1000\right)\ Pr_{2,3}}{1 + 12.7\left[\frac{f_{2,3}}{8}\right]^{(1/2)}\left[Pr_{2,3}^{(2/3)} - 1\right]} \tag{19}$$

The convective coefficient is obtained by the equation (Incropera et al., 2008):

$$H_{2,3} = Nu_{2,3}\frac{k_{R\,2,3}}{d_c} \tag{20}$$

3.2.2. Two-phase flow segment

Convective coefficient $H_{3,4}$, the area of the exchanger $A_{3,4}$, and the length of the exchanger $L_{3,4}$ were determined from the correlation of Shah, (2017), which is an update of the correlation of Shah, (1982). The two-phase convective coefficient given by the Shah correlation, (2017) is the maximum value of the equation:

$$H_i = Máx\begin{Bmatrix} 1.8\ B_1^{-0.8}\ B_3 H_l \\ 230\ Bo^{0.5}\ B_3 H_l \\ B_2\ Bo^{0.5}\ exp\left(2.74\ B_1^{-0.1}\right) B_3 H_l \\ B_2\ Bo^{0.5}\ exp\left(2.74\ B_1^{-0.15}\right) B_3 H_l \end{Bmatrix} \tag{21}$$

From which we have the values of the constants B_1, B_2 and B_3:

$$B_1 = \begin{Bmatrix} Co\ \ if\ horizontal\ with\ Fr_l \geq 0.04\ or\ vertical \\ 0.38\ Co\ Fr_l^{-0.3}\ \ if\ horizontal\ with\ Fr_l < 0.04 \end{Bmatrix} \tag{22}$$

$$B_2 = \begin{Bmatrix} 14.7, \quad if\ Bo \geq 0.0011 \\ 15.4, \quad if\ Bo < 0.0011 \end{Bmatrix} \tag{23}$$

$$B_3 = \begin{Bmatrix} 2.1 - 0.008\ We_v - 110\ Bo, \quad if\ B_3 \geq 1 \\ 1\ \ if\ B_3 < 1\ \ or\ \ Fr_l < 0.01 \end{Bmatrix} \tag{24}$$

Froud, Convection, and Weber numbers were calculated by the equations (Incropera et al., 2008):

$$Fr_l = \frac{G^2}{\rho_l^{\,2}\ g\ d_c} \tag{25}$$

$$Co = \left(\frac{1 - x}{x}\right)^{0.8}\left(\frac{\rho_v}{\rho_l}\right)^{0.5} \tag{26}$$

$$We_v = \frac{G^2 d_c}{\rho_v\ \sigma_c} \tag{27}$$

Heat transfer coefficient H_l was obtained from the Dittus-Boelter correlation (Incropera et al., 2008):

$$Nu_l = \frac{H_l\, d_c}{k_{Rc,c}} = 0.023\, Re_l^{0.8} \; - \; Pr_l^{0.4} \tag{28}$$

These dimensionless were calculated from the thermodynamic properties of the fluid in the heat exchanger for the saturated vapor states, such as specific mass ($\rho_{c,v}$ = 15.53 kg/m^3) and for the saturated liquid state, such as specific heat (cp_l = 2.591 kJ/kg-K), specific mass ($\rho_{c,l}$ = 523.1 kg/m^3), thermal conductivity ($k_{R,c,c}$ = 0.082 W/m-K), surface tension (σ_c = 0.007646 N/m), kinematic viscosity ($\mu_{c,l}$ = 0.00012 kg/m-s) and enthalpy of vaporization ($h_{c,lv}$ = 305.1 kJ/kg). Convective coefficient $H_{3,4}$ was obtained by averaging 10 regular intervals varying enthalpy from h_3 to h_4.

3.2.3. Subcooled liquid segment

Convective coefficient $H_{4,5}$, area of the heat exchanger $A_{4,5}$, and the length of the exchanger $L_{4,5}$ were determined by calculating the Reynolds ($Re_{c,4,5}$ = 2408) and Prandtl ($Pr_{c,4,5}$ = 3.851) obtained from the mass flow rate and thermodynamic properties of the fluid in the heat exchanger such as specific heat ($cp_{4,5}$ = 2.571 kJ/kg-K), thermal conductivity ($k_{R4,5}$ = 0.0829 W/m-K) and friction factor ($f_{4,5}$ = 0.0264). Gnielinski's correlation as in Eq. (19) was chosen as the most appropriate to calculate the global coefficient and the convective coefficient, covering a wide range of Reynolds values (Incropera et al., 2008).

The convective coefficient was obtained by the equation (Incropera et al., 2008):

$$H_{4,5} = Nu_{4,5}\, \frac{k_{R\,4,5}}{d_c} \tag{29}$$

3.2.4. Results

The values of the convective coefficients found in each segment allowed the calculation of the area and length of the heat exchanger:

Table 03. Condenser Results.

	Segment 2-3	Segment 3-4	Segment 4-5	Total
Nusselt (*Nu*)	54.08	-	8.682	-
Convective coefficient (*H*)	378.6 W/m^2-K	524.2 W/m^2-K	239.8 W/m^2-K	-
Heat released to PCM (*Q*)	0.0423 kJ/s	0.2148 kJ/s	0.009 kJ/s	0.266 kJ/s
Condenser area (*A*)	0.0037 m^2	0.0254 m^2	0.00254 m^2	0.0297 m^2
Length (*L*)	0.395 m	2.691 m	0.270 m	3.355 m

Heat exchange varied 15% less than that specified by the manufacturer's manual. This difference is attributed to the diameter of the condenser, which used the value proposed by Yuan and Cheng, (2014).

3.3. Capillary tube

From inlet and outlet pressures of the capillary tube, and considering the process as isenthalpic:

Table 04. Fluid properties at the capillary tube inlet (5) and capillary tube outlet (6).

Property	Capillary tube inlet (5)	Capillary tube outlet (6)
Pressure (*P*)	604.0 kPa	72.2 kPa
Specific Volume (*v*)	0.0019 m^3/kg	0.1856 m^3/kg
Enthalpy (*h*)	297.1 kJ/kg	297.1 kJ/kg

Considering capillary tube diameter (d_{cap} = 0.0004 m) were calculated the friction factor (f_{cap} = 0.018) and mass velocity (G = 5603 kg/s-m^2). The capillary tube length (L_{cap} = 0.142 m) was calculated by the sum of sub-cooled length (L_{sub} = 0.055 m) and two-phase length (L_{2f} = 0.087 m) sections.

3.4. Evaporator

Vaporization temperature was set at -20.0°C according to Embraco, (2022) and was considered a constant pressure along the heat exchanger (isobaric). The internal diameter of the evaporator (d_e) arbitrated was 0.003 m (Yuan and Cheng,

2014). At point (6) the refrigerant fluid was considered in the two-phase state, at point (7) in the saturated vapor state and at point (1) in the superheated vapor state, from the superheat arbitration of 7.0 °C:

Table 05. Fluid properties at the relevant points of the evaporator.

Property	Evaporator inlet (6)	Saturated vapor (7)	Evaporator outlet (1)
Pressure (P)	72.2 kPa	722 kPa	72.2 kPa
Temperature (T)	-20.0 °C	-20.0 °C	-13.0 °C
Enthalpy (h)	297.1 kJ/kg	528.4 kJ/kg	539.0 kJ/kg
Quality (x)	0.38	1	-

3.4.1. Two-phase flow segment

Convective coefficient $H_{6,7}$, the area of the exchanger $A_{6,7}$, and the length of the exchanger $L_{6,7}$ were determined from the correlation of Shah, (2017), which is an update of the correlation of Shah, (1982). The two-phase convective coefficient given by the Shah correlation, (2017) is the maximum value of Eq. (21). Froud, Convection, and Weber numbers were calculated according to Eq. (25), Eq. (26), and Eq. (27) (Incropera et al., 2008). Heat transfer coefficient H_l was obtained from the Dittus-Boelter correlation (Incropera et al., 2008) in the same way as presented in Eq. (28). These dimensionless were calculated from the thermodynamic properties of the fluid in the heat exchanger for the saturated vapor states, such as specific mass ($\rho_{e,v}$ = 2.061 kg/m3) and for the saturated liquid state, such as specific heat (cp_l = 2.194 kJ/kg-K), specific mass ($\rho_{e,l}$ = 603.2 kg/m3), thermal conductivity ($k_{R,e,l}$ = 0.1067 W/m-K), surface tension (σ_e = 0.01521 N/m), kinematic viscosity ($\mu_{e,l}$ = 0.000253 kg/m-s) and enthalpy of vaporization ($h_{e,lv}$ = 373.4 kJ/kg). Convective coefficient $H_{6,7}$ was obtained by averaging 10 regular intervals varying enthalpy from h_6 to h_7.

3.4.2. Superheated vapor section

The convective coefficient $H_{7,1}$, exchanger area $A_{7,1}$ and length of exchanger $L_{7,1}$ were determined from the calculation of Reynolds ($Re_{e7,1}$ = 45979) and Prandtl ($Pr_{e,7,1}$ = 0.7703), obtained from the mass flow rate and thermodynamic properties of the fluid in the heat exchanger such as specific heat ($cp_{7,1}$ = 1.519 kJ/kg-K), thermal conductivity ($k_{R7,1}$ = 0.0128 W/m-K) and friction factor ($f_{7,1}$ = 0.0139). The Gnielinski correlation as in Eq. (19), was chosen as the most appropriate to calculate the global coefficient and the convective coefficient, covering a wide range of Reynolds values. The convective coefficient is obtained by Eq. (20) (Incropera et al., 2008).

3.4.3. Results

The values of the convective coefficients found in each segment allowed the calculation of the area and length of the heat exchanger:

Table 06. Evaporator Result

	Segment 6-7	Segment 7-1	Total
Nusselt (Nu)	-	65.77	-
Convective coefficient (H)	446.1 W/m^2-K	281.0 W/m^2-K	-
Heat absorbed (Q)	0.1629 kJ/s	0.007488 kJ/s	0.1704 kJ/s
Evaporator area (A)	0.03651 m^2	0.004583 m^2	0.041093 m^2
Length (L)	3.87 m	0.486 m	4.36 m

Heat exchange varied 10% less than that specified by the manufacturer's manual. This difference is attributed to the diameter of the condenser, which used the value proposed by Yuan and Cheng, (2014).

3.5. Phase Change Material

The minimum volume of the PCM (V_{PCM} = 0.00115 m^3) was calculated from PCM specific mass (ρ_{PCM} = 814.0 kg/m^3) and PCM latent heat (λ_{PCM} = 17.07 kJ/kg). If we consider the thickness of the PCM (δ_{PCM} = 0.005 m) and the width of the PCM ($L1_{PCM}$ = 0.4 m), the length necessary for absorbing the heat of the condenser ($L2_{PCM}$ = 0.57 m) is obtained.

3.6. Coefficient of Performance

The coefficient of performance (COP = 1.778) was obtained from the ratio between the heat absorbed in the evaporator ($\dot{Q}_{evap}$ = 0.1704 kJ/s) and the work done by the compressor ($\dot{W}_{comp}$ = 0.0958 kJ/s). COP varied 26% higher than that

specified by the manufacturer's manual. This difference is attributed to the work done by the compressor because of the consideration that the compressor would not exchange heat with the environment.

4. CONCLUSION

The variation of heat exchange observed on the condenser and evaporator compared to that specified by the manufacturer's manual was attributed to the diameter of the condenser, which used the value proposed by Yuan and Cheng, (2014). The difference is attributed to the work done by the compressor, considering that the compressor would not exchange heat with the environment.

From the calculations performed on the mathematical model of the refrigerator, the use of PCM in the condenser directly impacts the value of the COP and is viable for implementation in domestic refrigerators, contributing to the reduction of energy used for food conservation.

5. ACKNOWLEDGEMENTS

We thank FAPEMIG (The Minas Gerais Research Funding Foundation), CAPES (Coordination for the Improvement of Higher Education Personnel), and CNPQ (National Council for Scientific and Technological Development).

6. REFERENCES

Azzouz, K., Leducq, D. and Gobinb, D., 2008. "Performance enhancement of a household refrigerator by addition of latent heat storage". *International Journal of Refrigeration* No 31, pp 892-901.

Bakhshipour, S., Valipour, M.S. and Pahamli, Y., 2017. "Parametric analysis of domestic refrigerators using PCM heat exchanger*". International Journal of Refrigeration* No 83, pp 1–13.

Boeng, J. and Melo, C., 2014. "Mapping the energy consumption of household refrigerators by varying the refrigerant charge and the expansion restriction". *International Journal of Refrigeration* No 41, pp 37-44.

Cheng, W. and Yuan, X., 2013. "Numerical analysis of novel household refrigerator with shape-stabilized PCM (phase change material) heat storage". *Energy* No 59, pp 265–276.

Embraco, 2022. "*EM2T60CLP Datasheet*" Embraco Nidec Global Appliance. 26 Mar. 2022 <https://www.embraco.com/>.

Incropera, F. P., Dewitt, D. P., Bergman, T. L. and Lavine, A. S., 2008. *Fundamentos de transferência de Calor e de Massa*. LTC, Rio de Janeiro, 6th edition.

Joybari, M. M., Hatamipour, M. S., Rahimi, A. and Modarres, F. G., 2013. "Exergy analysis and optimization of R600a as a replacement of R134a in a domestic refrigerator system". *International Journal of Refrigeration* No 36, pp 1233-1242.

Joybari, M. M., Haghighata, F., Moffatb, J. and Sraba, P., 2015. "Heat and cold storage using phase change materials in domestic refrigeration systems: The state-of-the-art review". *Energy and Buildings* No 106, pp 111–124.

Marques, A., Davies, G., Maidment, G., Evans, J., and Wood, I., 2014. "Novel design and performance enhancement of domestic refrigerators with thermal storage", *Applied Thermal Engineering* No 63, pp 511–519.

Shah, M. M., 1982. "Improved general correlation for critical heat flux in uniformly heated vertical tubes". *International Journal Heat and Fluid Flow* No 8, pp 326-335.

Shah, M. M., 2017. "Unified correlation for heat transfer during boiling in plain mini/micro and conventional channels". International Journal of Refrigeration No 74, pp 606-626.

Sonntag, R. E., Borgnakke, C., 2003. *Introduction to Engineering Thermodynamics*. LTC, Rio de Janeiro, 1st edition.

Wang, F., Maidment, G., Missenden, J. and Tozer, R., 2007. "The novel use of phase change materials in the refrigeration plant. Part 2: Dynamic simulation model for the combined system". *Applied Thermal Engineering* No 27, pp 2902-2910.

Yuan, X. D., Cheng, W. L., 2014. "Multi-objective optimization of household refrigerator with novel heat-storage condensers by Genetic algorithm". *Energy Conversion and Management* No 84, pp 550-561.

7. RESPONSIBILITY NOTICE

The authors are the only ones responsible for the printed material included in this paper.